

Article

Evaluating the Differences in Modeling Biophysical Attributes between Deciduous Broadleaved and Evergreen Conifer Forests Using Low-Density Small-Footprint LiDAR Data

Yoshio Awaya ^{1,*} and Tomoaki Takahashi ^{2,*}

¹ River Basin Research Center, Gifu University, 1-1 Yanagido, Gifu 501-1193, Japan

² Kyushu Research Center, Forestry and Forest Products Research Institute, 4-11-16 Kurokami, Chuo-ku, Kumamoto 860-0862, Japan

* Correspondence: awaya@green.gifu-u.ac.jp (Y.A.); tomokun@ffpri.affrc.go.jp (T.T.)

Academic Editors: Lalit Kumar, Onisimo Mutanga, Lars T. Waser and Randolph H. Wynne

Received: 15 March 2017; Accepted: 5 June 2017; Published: 7 June 2017

Abstract: Airborne light detection and ranging (LiDAR) has been used for forest biomass estimation for the past three decades. The performance of estimation, in particular, has been of great interest. However, the difference in the performance of estimation between stem volume (SV) and total dry biomass (TDB) estimations has been a priority topic. We compared the performances between SV and TDB estimations for evergreen conifer and deciduous broadleaved forests by correlation and regression analyses and by combining height and no-height variables to identify statistically useful variables. Thirty-eight canopy variables, such as average and standard deviation of the canopy height, as well as the mid-canopy height of the stands, were computed using LiDAR point data. For the case of conifer forests, TDB showed greater correlation than SV; however, the opposite was the case for deciduous broadleaved forests. The average- and mid-canopy height showed the greatest correlation with TDB and SV for conifer and deciduous broadleaved forests, respectively. Setting the best variable as the first and no-height variables as the second variable, a stepwise multiple regression analysis was performed. Predictions by selected equations slightly underestimated the field data used for validation, and their correlation was very high, exceeding 0.9 for coniferous forests. The coefficient of determination of the two-variable equations was smaller than that of the one-variable equation for broadleaved forests. It is suggested that canopy structure variables were not effective for broadleaved forests. The SV and TDB maps showed quite different frequency distributions. The ratio of the stem part of the broadleaved forest is smaller than that of the coniferous forest. This suggests that SV was relatively smaller than TDB for the case of broadleaved forests compared with coniferous forests, resulting in a more even spatial distribution of TDB than that of SV.

Keywords: stem volume; dry biomass; conifer; broadleaves; light detection and ranging (LiDAR); regression analysis; correlation coefficient

1. Introduction

Biomass and stem volume (SV) are important variables for forestry and carbon balance studies. The biomass and carbon stocks in forests are important indicators of their productive capacity, energy potential, and capacity to sequester carbon [1]. Biomass is a pool of atmospheric carbon fixed by plants and ranges widely based on tree size in large areas. Stem volume (SV) is basic piece of information for informing lumber production in forest management. The stem volume of a tree is the principal commercial product of forests as the stem contains a large proportion of the biomass of a tree [2].

Airborne laser technology was introduced for forest measurements in the early 1980s, and a laser profiler revealed that, in a large area, tree canopy height was measurable from the air [3,4]. Large-area forest inventory is a time-consuming task; however, biomass estimation using light detection and ranging (LiDAR) point data has become popular for creating wall-to-wall inventories. LiDAR-based inventories have been recognized as essential in providing more accurate estimates of biophysical properties than conventional methods. Although airborne laser observation and data processing is costly, it provides forest resource information over large areas with wall-to-wall coverage. Further, the use of laser data for forest inventories has shown promising results with improved accuracies [5]. Various studies have since been executed to evaluate the performance of airborne laser sensors for evaluating forest variables, such as SV and above-ground biomass (AGB) of pine [6], AGB of deciduous broadleaved [7] and evergreen coniferous [8] forests, and SVs of spruce and pine forests [9]. The improvement of LiDAR technology in the field of pulse density and accurate positioning [5] yields accurate small-footprint laser data, which are applicable for precise biomass mapping [10,11].

Various LiDAR variables have been examined and found to be useful for SV or biomass estimation by many scientists [10,12–15]. However, variable effectiveness and estimation accuracy differ as a function of footprint size [14], point density [15], scan angle [11], tree size, and canopy structure [16]. LiDAR data are also suitable for biophysical variable estimation, such as tree density and canopy height [17]. LiDAR data show strong coefficients of determination that mostly exceed 0.85 for logarithmic equations of various stand variables, including SV and AGB in a hardwood forest [18]. Separating areas with different forest types is essential to improve the accuracy of biomass mapping using LiDAR data [19], since individual analyses of different forest types improves the prediction accuracy of forest variables [20,21]. LiDAR-derived forest structure variables, such as canopy height, DBH, and AGB are used for large-area biomass mapping using high-resolution satellite data, since LiDAR data provides accurate stand information as reference data in a large area [22]. Above all, Næsset [5] pointed out that LiDAR-derived height variables, other than the maximum canopy height, was influenced little by pulse density even in the case of low-density data between 0.25 and 1.13 pulses m^{-2} . Thus, low-density LiDAR data could provide accurate canopy height information, and studying the performance of low-density small-footprint LiDAR data remains important and worth analyzing.

Tsuzuki et al. [23] pointed out that SV is theoretically proportional to the space between the canopy surface and the ground (hereafter, canopy space). The average canopy height is determined by the canopy space divided by the stand area. Thus, the canopy space and average canopy height are identical and the average canopy height will be useful for SV estimation. However, individual tree analysis has become popular for variables, such as tree height [24], AGB, and SV. Some recent research has focused on double-logarithmic relationships, especially for single tree analysis, between AGB or SV and variables that are derived from LiDAR data, including the average canopy height [12,25,26]. Alternatively, areal-based analysis produces better results than individual tree-based analysis for SV and AGB [26]. Although various studies have been conducted, most were stand-level studies. Therefore, it is important to evaluate the causes of the estimate variation in the stand-level analysis prior to operational use [27].

Most LiDAR-based studies separately analyzed the biomass of conifer, broadleaved, or mixed forests [6–10,12–18,25,28]. Therefore, the difference in LiDAR data performance in biomass estimation between evergreen coniferous and deciduous broadleaved forests [21] is one of interest in temperate zones, since evergreen coniferous and deciduous broadleaved forests are the dominant forest types. The performance of LiDAR data for biomass estimation is probably different among forest types [21]. Understanding the difference, and its cause in the estimation of SV and dry biomass, such as AGB and total dry biomass (TDB) by forest types, are essential to improve estimation methods. Although SV and TDB are indicators of biomass, they show tree biomass with different measures, volume of the stem part, or the dry weight of whole tree, respectively. Therefore, biomass of coniferous and broadleaved forests would be evaluated differently.

The aims of this study were to (1) identify LiDAR variables which have high correlations with SV, AGB, and TDB; (2) produce TDB and SV estimation models by multiple regression analysis using 38 LiDAR variables; and (3) validate the accuracy of TDB and SV estimation. The primary objective is identifying useful LiDAR variables for TDB and SV estimation in evergreen coniferous and deciduous broadleaved forests. Finding the difference in useful LiDAR variables between SV and TDB estimation is also an important objective. The resultant TDB and SV maps were compared to determine the relative difference of SV and TDB distributions caused by their definition.

2. Materials and Methods

2.1. Study Area

The study area is located in the Daihachiga river basin in Takayama City, Gifu in Central Japan between 36.16166°N, 137.32676°E (northeastern corner) and 36.13238°N, 137.44865°E (southwestern corner, Figures 1 and 2) in a cool temperate zone. The elevation ranges between 650 and 1600 m above sea level (ASL) with a steep topography and an average slope angle of 30°. The mapping extent covers a mountainous 8.3 km (east to west) by 2.0 km (north to south) area (36.14393°N, 137.40165°E at the center, Figure 2).

According to local information, most of the river basin was completely logged about 60–70 years ago after World War II and, therefore, the forests in this study site are considered relatively young. Planted forests of evergreen conifers, which include Japanese cedar (*Cryptomeria japonica* D. Don) and hinoki cypress (*Chamaecyparis obtusa* Sieb. et Zucc.), are dominant in the area below approximately 1000 m ASL. Some hinoki cypress stands are mixed with Japanese cedar. Planting Japanese cedar was most common around the 1950s to 1960s, because Japanese cedar is a fast-growing species for timber production used for the restoration of buildings after damage from World War II. Hinoki cypress was introduced around the 1970s to 1990s because of its valuable commercial quality [29]. Japanese cedar was also planted recently. Therefore, the ages of Japanese cedar and hinoki cypress stands are clearly different in the study area. Natural deciduous broadleaved forests dominate in areas above 1000 m ASL, and planted Japanese larch (*Lalix leptolepis* Gordon) forests exist in areas above 1200 m ASL. The dominant deciduous broadleaved species in this region are deciduous oak (*Quercus mongolica* var. *grosseserrata* Rehder et Wilson), Japanese white birch (*Betula platyphylla* var. *japonica* Hara), Erman's birch (*Betula ermanii* Cham.), and the dominant species vary with elevation and successional stages of stands. Japanese larch was planted around the 1950s for a short period, and the tree size is similar among larch stands. Therefore, larch was not analyzed in this study. Models for deciduous broadleaved forests were used to map SV and TDB for larch stands.

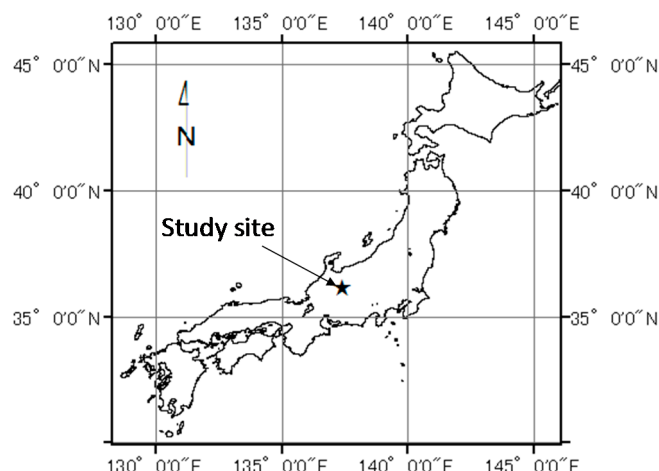


Figure 1. Location of the study site.

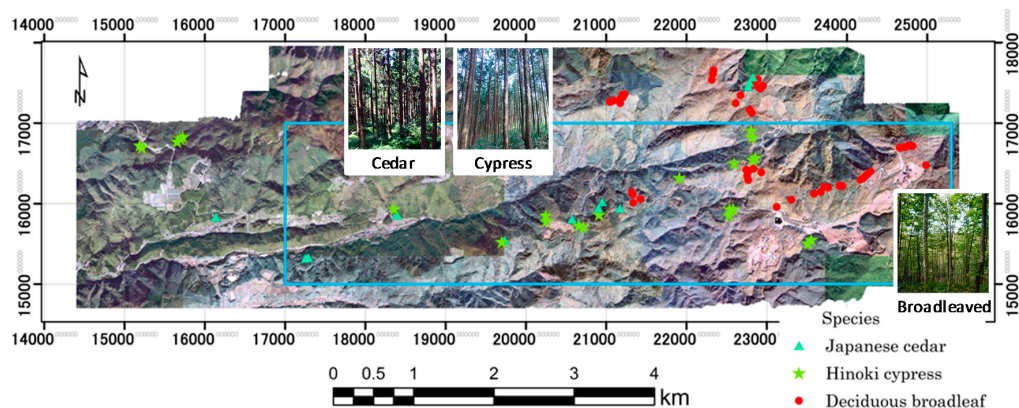


Figure 2. Plot location map. The orthophoto shows the common coverage of three light detection and ranging (LiDAR) data. The blue square area represents the location of the resulting maps of TDB and SV. The three photos show typical stands in the study site. The coordinate system of the map is Japan Plane Rectangular Coordinate System VII. Deciduous trees that had dropped leaves at the time of photo acquisition in 2012 appear in orange.

2.2. Sample Plots

Plot surveys were undertaken between 2010 and 2013 for deciduous broadleaved trees, Japanese cedar, and hinoki cypress. Sample plot areas were selected using aerial orthophotos and in situ field verification in advance of the field surveys for the following reasons: Since forest size distribution was uneven, it was difficult to find juvenile and old stands in the study area. Plots were selected along forest roads, but further than 10 m from the road side in order to facilitate the location identification on the aerial orthophotos, as well as to reduce access time to the plots. Plots were selected on graded slopes to minimize the effects of topographical accuracy differences in digital terrain models (DTM). Various height classes of stands were selected for the surveys, and circular plots were set in relatively homogeneous parts of stands. Plot radii varied between 5 and 17 m based on tree height and tree density in order to control the number of sample trees in a plot. Plot radius was determined to be large enough to include at least 40 sample trees. Stem diameter (cm) at 1.2 m DBH height and 4 cm minimum diameter of all trees was measured using calipers. The circular plot was divided into four quadrants for the convenience of tree identification. Since trees were very small and numerous, the DBH of all trees was measured in one quadrant of juvenile stands of which the top layer height was less than approximately 5 m. Tree height (H , m) was measured using a Vertex hypsometer (Haglöf, Avesta, Dalarnas, Sweden) for all trees for which DBH was measured.

A stake was set at the center of each plot, and plot center location was determined using a GPS receiver (either Mobile Mapper CX or Mobile Mapper 100 receivers, Thales, Arlington, VA, USA) with an external antenna by recording for at least 30 min by post-differential GPS (Figure 2). Plot coordinates were also checked on the aerial orthophotos (see the next sub-section). If the coordinate was uncertain based on the aerial orthophotos interpretation, coordinates were re-measured up to two times using the Mobile Mapper 100 receiver in the field until the location was confirmed on the aerial orthophotos.

During the four years, 12, 23, and 55 sample plots were measured for Japanese cedar, hinoki cypress, and broadleaved stands, respectively (Figure 2). Stem volume (SV, m^3) was calculated using DBH, H of sample trees, and the volume equations for Japanese cedar, hinoki cypress, deciduous broadleaved trees, and larch. These equations were modeled by the Nagoya Regional Forestry Office of the Japanese Forestry Agency [30–33]. Dry above- and below-ground biomass (AGB and BGB, respectively) of each tree were calculated using DBH, specific gravity of the wood for each species, and allometric equations for AGB and BGB [34]. SV ($m^3 ha^{-1}$), AGB ($Mg ha^{-1}$) and BGB ($Mg ha^{-1}$) of each plot were computed. Total dry biomass ($Mg ha^{-1}$, TDB) was computed by summing AGB and BGB. The survey results are summarized in Table 1.

Table 1. Summary of sample plot surveys.

Forest Type	No of Plots	Average DBH (cm)	Average Tree H (m)	Stem Volume ($m^3 \text{ ha}^{-1}$)	Above Ground Biomass ($Mg \text{ ha}^{-1}$)	Total Dry Biomass ($Mg \text{ ha}^{-1}$)
Japanese cedar *	4	1.1–9.4	1.8–5.8	2.4–80.9	1.9–67.5	2.6–86.1
	8	22.6–41.2	18.8–29.1	619.5–1068.3	273.8–384.6	325.7–467.1
Hinoki cypress *	21	14.6–34.3	9.6–21.4	106.6–555.7	98.8–281.0	110.4–444.9
Deciduous Broadleaved	5	1.1–25.7	1.7–21.3	6.2–408.7	4.9–263.0	7.2–317.6

* Planted tree species have been changed from cedar, cypress to cedar in conifer plantations.

2.3. Aerial Orthophotos and Forest Type Map

Three sets of aerial orthophotos with 50 cm pixels taken in June 2003, September 2008, and November 2012 (Figure 2), were supplied by the government of Gifu Prefecture and used as the reference for plot location, surveys, and location validation of the GPS measurements. For analysis, we used a forest-type map (Figure 3) [35], which was created by a decision-tree classification procedure using QuickBird images that were obtained in 2007, and a digital canopy height model based on LiDAR data, which was obtained in 2003. Forests were classified into three types in the map: evergreen coniferous forests (Japanese cedar and hinoki cypress), deciduous broadleaved forests, and larch forests. The forest type map was used to identify the forest-type distribution in biomass mapping. The forest-type map and orthophotos were geo-referenced to the Japan Plane Rectangular Coordinate System VII (JPRCS VII) with Japanese Geodetic Datum 2000 as raster images with 2.0 m pixels for the map and 0.5 m pixels for the photos.

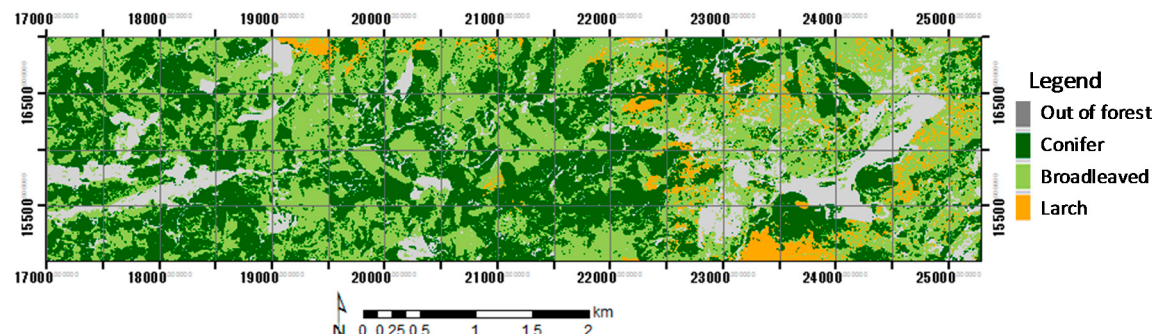


Figure 3. Forest type map of the mapping area.

2.4. Airborne LiDAR Data

The three airborne LiDAR datasets of the study area were obtained in October 2003, July 2005, and August 2011. The government of Gifu Prefecture supplied the 2003 LiDAR dataset. The geometric location of the data collected by airplanes or a helicopter was measured using a global positioning system and an inertial measurement unit. The point data were then geo-referenced to JPRCS VII. The footprint sizes of the three LiDAR datasets were between 0.2 and 0.4 m, and the point densities were 0.7, 1.8, and 1.0 pulses m^{-2} for the 2003, 2005, and 2011 LiDAR data, respectively. The LiDAR observations are summarized in Table 2.

Although the Gifu Prefecture government provided a 2 m raster DTM of the 2003 LiDAR data, the DTM was not accurate. For example, the terrain and canopy top showed the same elevation in very dense coniferous stands. Therefore we decided to produce a DTM using the three LiDAR datasets [36]. Elevations among the three LiDAR datasets were compared at six open areas, such as parking lots. The differences between the average of three, and each, LiDAR dataset were less than 10 cm. As a result, the elevation of the three LiDAR datasets was adjusted using these differences. The adjusted point data of the three LiDAR datasets were used in the following analysis including TDB and SV estimation.

Table 2. Summary of LiDAR observations.

Observation Date	Contractor	Scanner, Manufacturer	Beam Divergence (mrad)	Wave-Length (nm)	Flight Altitude Above Ground (m)	Foot-Print Size (m)	FOV (°)	Beam Density (pulse m ⁻²)	Usage
October 2003	Kokusai Kogyo Co., Chiyoda, Tokyo, Japan	RAMS, EnerQuest, Denver, CO, USA	0.33	1064	2000 (Entire Gifu Prefecture)	-	±22	0.7	DTM production
25 July 2005	Nakanihon Air Service Co., Nagoya, Aichi, Japan	ALTM 2050DC, Optech, Vaughan, Ontario, Canada	0.19	1064	1200	0.24	±22	1.8	DTM production
28 August 2011	Nakanihon Air Service Co.	VQ-580 RIEGL, Horn, Horn, Austria	0.50	1064	600	0.30	±30	1.0	Biomass estimation, DTM production

The three LiDAR point data were combined for the production of the DTM. Raster data of slope and Laplacian with a 7×7 pixel window were produced using the DTM from the 2003 LiDAR dataset using ERDAS Imagine 2011 (Hexagon Geospatial, Madison, AL, USA) as a reference. Low points were removed from the combined point data using Terra Scan (Terra Solid, Helsinki, Uusimaa, Finland). Terra Scan provided the ground function to select points hitting the ground using two parameters, angle and distance. We assumed that proper parameters differed as a function of terrain. Therefore, we separated the point data into three groups of mild slopes, steep slopes, and ridges. Areas where the Laplacian was greater than 90 with a slope greater than 20° were classified as ridges. Areas other than ridges where the slope was between 0° and less than 20° were classified as mild slopes. The remaining areas were classified as steep slopes. The angle and distance parameters of the ground function were set the 18° and 0.5 m, 18° and 2.5 m, and 30° and 5 m for mild slopes, steep slopes, and ridges, respectively. Ground point data were then selected for the three groups and combined. A revised DTM was produced using the selected ground points by TIN of ArcGIS 10 (ESRI, Redlands, CA, USA) as a 2 m raster image using JPRCS VII [36].

Of the three LiDAR datasets, the dataset obtained in August 2011 was used for the biomass study. Gridding of the digital canopy height model reduces height accuracy [37]. Therefore, the digital canopy height of the 2011 LiDAR first return points was computed as the difference between the elevation of each point and the interpolated terrain elevation at the point location using the 2 m raster DTM and the bi-linear interpolation method. Various LiDAR variables, shown in Table 3 and as described in the next sub-section, were computed using the digital canopy height for each plot for statistical analysis. A raster LiDAR variable file with a 10 m pixel size, which included the variables in Table 3 as channels, was produced for the entire test site in the same way as the calculation for plots for mapping of SV and TDB.

Table 3. Variables computed from LiDAR point data.

Target Points				Variables		
All points	Average height	Standard deviation	Coefficient of variance	Maximum height		Canopy closure
Points other than ground	Average height	Standard deviation	Coefficient of variance			
Points within canopy part	Average height	Standard deviation	Coefficient of variance	Height at every 10th percentiles	Height at every 10th part	Canopy closure at every 10th part

2.5. LiDAR Variables

Thirty-eight variables (Figure 4, Table 3), after Næsset [14], were calculated in order to evaluate the LiDAR-derived variables for the estimation of SV and TDB for planted evergreen coniferous forests (i.e., Japanese cedar and hinoki cypress forests) and natural deciduous broadleaved forests. Points were sampled from the area of each plot. Points over 0 m in the digital canopy height points were labeled as above-ground points. The canopy components were determined as follows: The average height and standard deviation (SD) of above-ground points were computed. The height which was two SDs below the average height was determined as the canopy bottom. Points above the canopy bottom were treated as returns from the canopy components. Average, SD, and coefficient of variance were

computed for all points, above-ground points, and points within the canopy. Fortran programs were written and used for the generation of digital canopy height points and LiDAR variable computation.

Variables are denoted as follows: maximum canopy height of the plot, Hmax; canopy closure, CC; average of all points, THavr; SD of all points, THsd; coefficient of variance of all points, THcv; above-ground point average, AHavr; above-ground point SD, AHsd; above-ground point coefficient of variance, AHcv; average of canopy points, CHavr; SD of canopy points, CHsd; coefficient of variance of canopy points, CHcv; height for each percentile (e.g., 10 percentile, H10%); each tenth of the canopy height (e.g., four-tenths, Hd4); and canopy closure at this height (e.g., C4). These variables were also computed as a 10 m raster image for biomass mapping, as described previously.

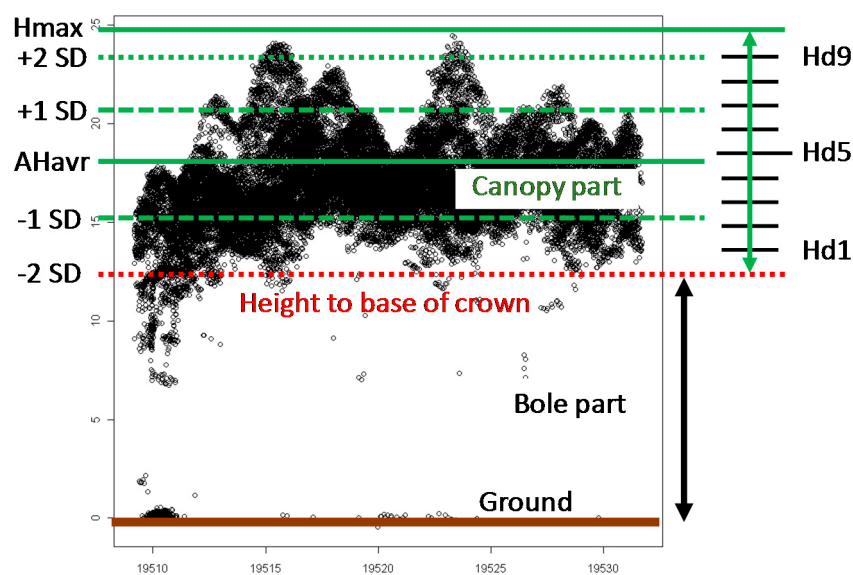


Figure 4. Graphical explanation of LiDAR variables. Hmax is the maximum canopy height, and AHavr and SD are the average height and the standard deviation of points above the ground in the plot, respectively. The height to base of the crown is defined as the height which is two SDs below AHavr. The canopy is defined as the part above the height to the base of the crown. Heights at every 10th percentile between 10% (H10%) and 90% (H90%) were computed. Heights (Hd1–9) and closures (C1–C9) at 10ths of the canopy heights between one-tenth (d1) and nine-tenths (d9) were also computed.

2.6. Correlation Analysis

Sample plots were separated into three groups (A, B, and C) by systematic sampling based on TDB for evergreen conifer stands and deciduous broadleaved stands separately. For example, the plot with the smallest TDB among coniferous or broadleaved stands was placed in group A, the plot with the second-smallest TDB was placed in group B, the plot with the third-smallest TDB was placed in group C, and the plot with the fourth-smallest TDB was placed in group A. This process was repeated for other plots. Thus, each group was composed of similarly-sized forests. Product-moment correlation coefficients between SV and the LiDAR data variables were separately computed for evergreen coniferous and deciduous broadleaved forests for all sample plots and for each group of sample plots. Scores were given to variables to evaluate the suitability of variables for biomass estimation as follows: three points to the variable with the greatest correlation, two points to the variable with the second-greatest correlation, and one point to the variable with the third-greatest correlation in the sample sets described above. The points were summed for each variable to identify variables that were less affected by sample combinations for biomass estimation.

2.7. Regression Analysis

A multiple regression analysis by a step-up procedure using Bayesian information criterion for variable selection was applied to the evergreen coniferous and deciduous broadleaved datasets separately using JMP ver. 11 (SAS Institute Inc., Cary, NC, USA). Three combinations were tested for each of the three groups for coniferous and broadleaved forests. Samples of two groups, such as groups A and B, were used for modeling, and samples in the other group, such as group C, were used for validation. Regression models with one and two variables were built. If a canopy height variable was selected as the first variable, only variables other than height, such as canopy structure variables, like canopy closure or SD of canopy height, were used for the second variable selection. Coefficients of determination of equations were compared among the three groups, and the equation with the greatest coefficient of determination was selected as the best model for SV and TDB mapping.

Maps of SV and TDB were produced using the raster LiDAR variable file, forest type map, and selected models using a program we developed in Fortran. A model for deciduous broadleaved forests was used for larch forests based on the results of a comparison of estimates using models for conifer and broadleaved forests. Biomass distribution patterns were visually evaluated using the SV and TDB maps. Frequency histograms of TDB and SV were drawn, and their features were visually evaluated. A scattergram between TDB and SV of field plots was examined to infer the cause of the spatial pattern differences between the TDB and SV distribution maps.

ERDAS Imagine 2010 (Hexagon Geospatial, Madison, AL, USA) was used for raster data conversion, and ArcGIS 10 was used for map creation.

3. Results

3.1. Correlation Coefficients

Correlation coefficients greater than approximately 0.9 appeared in AHavr for SV, AGB, and TDB for conifer stands, with a score of 18 points (Table 4). Thus AHavr was the most effective variable for biomass estimation for this dataset. Alternatively, the mid-height between four- and six-tenths of the canopy of deciduous broadleaved forests (Hd4, Hd5, and Hd6) had correlation coefficients greater than approximately 0.85 for the three biomass variables with scores greater than 13 (Table 5). Although the mid-canopy height showed high correlation, the height ranged rather broadly. Tables 4 and 5 shows variables with higher points among LiDAR variables. Correlation coefficients were almost the same between LiDAR variables and AGB or TDB in Table 4. All correlation coefficients in Tables 4 and 5 were significant ($p < 0.01$).

Table 4. Correlation coefficients between LiDAR and stand variables—Evergreen conifer (n = 35).

LiDAR	Volume ($\text{m}^3 \text{ ha}^{-1}$)	AGB (Mg ha^{-1})	TDB (Mg ha^{-1})	Score *
Hd4	0.871	0.915	0.915	6
Hd5	0.876	0.912	0.912	8
Hd6	0.874	0.904	0.903	7
AHavr	0.894	0.915	0.913	18
H40%	0.886	0.900	0.896	7

* Score is an evaluation of correlation coefficients. Correlation coefficients that were the greatest, second, or third highest among the LiDAR variables were given 3, 2, and 1 points, respectively, for four cases of correlation calculations and summed. Since relationships between biomass and LiDAR-derived variables vary by samples, the general trend was evaluated by the score.

Table 5. Correlation coefficients between LiDAR and stand variables—Deciduous Broadleaved ($n = 55$) forests.

LiDAR	Volume ($\text{m}^3 \text{ ha}^{-1}$)	AGB (Mg ha^{-1})	TDB (Mg ha^{-1})	Score *
Hd4	0.912	0.854	0.852	16
Hd5	0.912	0.856	0.854	14
Hd6	0.909	0.857	0.854	13
AHavr	0.907	0.843	0.840	0
H40%	0.904	0.839	0.836	0

* Score is an evaluation of correlation coefficients. Correlation coefficients that were the greatest, second, or third highest among the LiDAR variables were given 3, 2, and 1 points, respectively, for four cases of correlation calculations and summed. Since relationships between biomass and LiDAR-derived variables vary by samples, the general trend was evaluated by the score.

3.2. Regression Analysis and Validation

The following equations were derived by regression analysis:

One-variable equations:

Evergreen coniferous forest:

$$\text{SV} = 43.0 \times \text{AHavr} - 171.3 \quad (1)$$

$$\text{TDB} = 18.3 \times \text{AHavr} - 1.3 \quad (2)$$

Deciduous broadleaved forest:

$$\text{SV} = 16.3 \times \text{Hd5} - 53.6 \quad (3)$$

$$\text{TDB} = 12.0 \times \text{Hd5} - 21.1 \quad (4)$$

The coefficients of determination adjusted for the degrees of freedom were 0.859, 0.896, 0.821, and 0.739 for Equations (1)–(4), respectively.

Two-variable equations:

Evergreen conifer forest:

$$\text{SV} = 55.2 \times \text{AHavr} + 825.4 \times \text{CHcv} - 482.4 \quad (5)$$

$$\text{TDB} = 18.5 \times \text{AHavr} - 216.0 \times \text{C8} + 12.2 \quad (6)$$

Deciduous broadleaved forest:

$$\text{SV} = 17.9 \times \text{Hd5} + 1281.4 \times \text{CC} - 1324.8 \quad (7)$$

$$\text{TDB} = 12.5 \times \text{Hd5} - 107.0 \times \text{C7} - 7.5 \quad (8)$$

where C7 and C8 (no units) are canopy closures at seven- and eight-tenths of the canopy height, CHcv is the coefficient of variance of the LiDAR points returning from canopies, and CC is the canopy closure (no units). The coefficient of C8 in Equation (6) was not significant ($p > 0.05$); however, the other coefficients were significant ($p < 0.05$). The coefficients of determination adjusted for the degrees of freedom were 0.903, 0.903, 0.849, and 0.762 for Equations (5)–(8), respectively. The numbers of samples were 22 for coniferous forests and 38 for deciduous broadleaved forests, and all eight equations were significant ($p < 0.0001$). High coefficients of determination were observed especially for Equations (2), (5), and (6) for SV and TDB of conifer stands. Although the coefficients of determination of the broadleaved forest were smaller than those of coniferous forest, the equations for SV estimation had a high coefficient of determination. These equations could provide accurate biomass estimates.

Validation results showed that predicted volume tended to be slightly underestimated based on the regression lines between field measurements and the predictions by the equations for SV and TDB. Slopes were between 0.928 and 0.971 (Figures 5 and 6). In particular, volume predictions tended to be slightly underestimated in dense Japanese cedar stands with high volume, and slightly overestimated in hinoki cypress stands with relatively low density. The models for conifer forests might underestimate the true Japanese cedar volume and overestimate the true hinoki cypress volume. Models should be developed for each species separately [20,21]. Japanese cedar trees had a multilayer structure because of intraspecies competition due to unthinned conditions. Understory trees were invisible from the air, since the upper canopy covered them. Therefore, the biomass estimate was relatively low, because the understory was not evaluated in the overall estimation using upper layer canopy information. On the other hand, almost all hinoki cypress stands had a uniform one-layer canopy and relatively low biomass, resulting in an overestimate using the canopy information. Thus, canopy structure influences the biomass estimates [38]. The standard errors (SEs) for volume validation (Figure 5) were 140.9 and 126.8 $\text{m}^3 \text{ ha}^{-1}$ for one- and two-variable equations for coniferous forests, respectively. The SEs were 32.3 and 37.1 $\text{m}^3 \text{ ha}^{-1}$ for one- and two-variable equations for broadleaved forests, respectively. For TDB (Figure 6), the SEs were 49.0 and 47.6 Mg ha^{-1} for one- and two-variable equations for coniferous forests, respectively, and 35.8 and 36.0 Mg ha^{-1} for one- and two-variable equations for broadleaved forests, respectively.

In the validation results, SEs of the two-variable equations were worse or almost equal to those of one-variable equations for SV and TDB of broadleaved forests. Samples for modeling and validation were different, and the results suggest the following: The models were built to minimize residuals among the modeling plots by the least square method. The no-height variable was set in order to reduce canopy structure difference. However, the canopy shape of broadleaved trees is irregular and differs tree by tree. Therefore, the canopy structure was different among the sample plots and between modeling and validation sample groups. Although the second variable was set to reduce residuals in the modeling group, it was not effective for broadleaved forests.

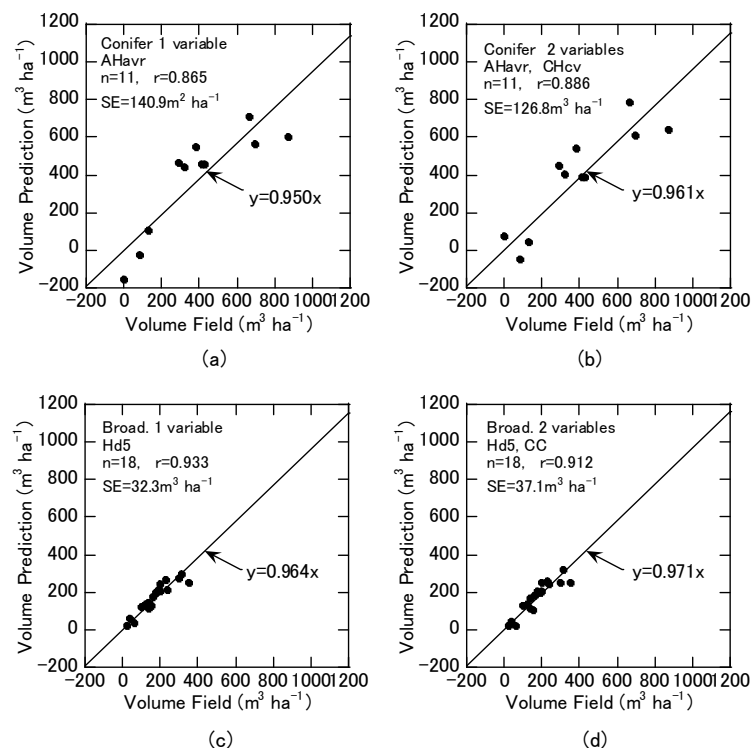


Figure 5. Validation results of SV prediction based on comparison of predicted and field SV. (a) One- and (b) two-variable models for evergreen coniferous forests, and (c) one- and (d) two-variable models for deciduous broadleaved forests.

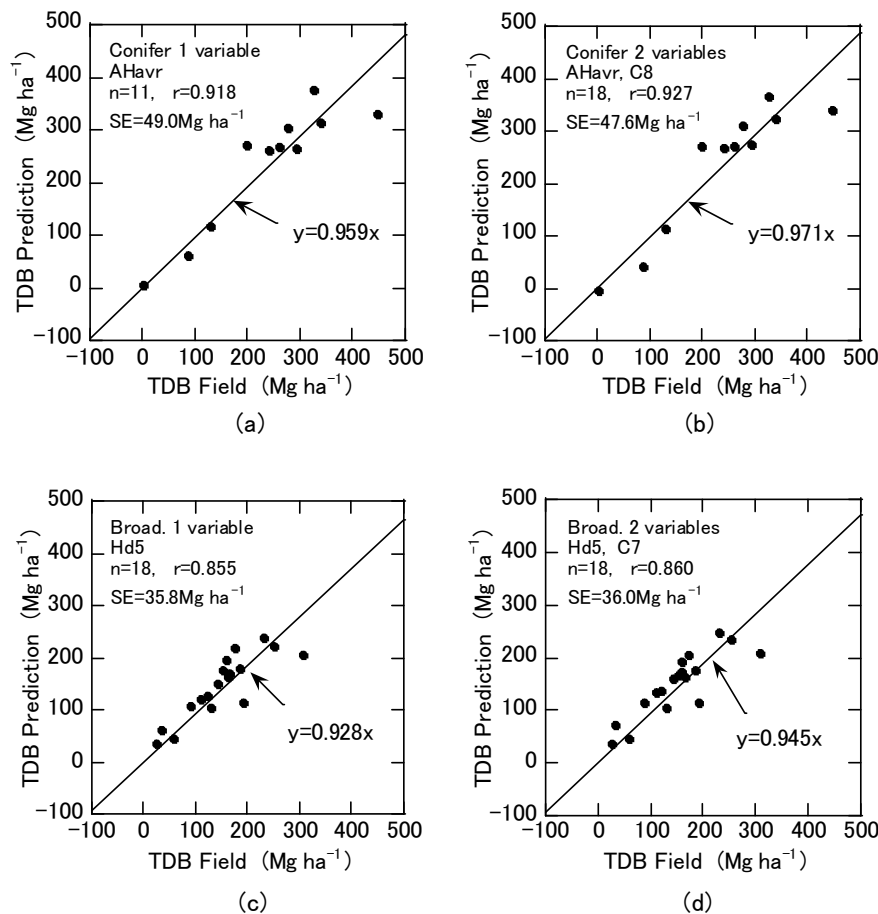


Figure 6. Validation results of TDB prediction based on the comparison of predicted and field TDB. (a) One- and (b) two-variable models for evergreen conifer forests, and (c) one- and (d) two-variable models for deciduous broadleaved forests.

3.3. Biomass Distribution

According to the plot survey, the SVs of broadleaved and conifer stands reached 400 and $1000 \text{ m}^3 \text{ ha}^{-1}$, respectively (Table 1). Forest owners have not cared for their forests for decades, and many mature Japanese cedar stands were not thinned. Japanese cedar is relatively older than hinoki cypress and is a fast-growing species. Dense, mature Japanese cedar stands with high SV exist in the study site.

Figure 7 shows forests with high SV in the mapping area. A small village was located to the left (west) of the mapping area, and planted evergreen coniferous forests were common (Figure 3). Areas with high SV in the west mainly included mature Japanese cedar forests. However, there were no villages in the eastern two-thirds of the mapping area, and broadleaved and young coniferous forests dominated. Therefore, the SVs of these forests were small, less than $500 \text{ m}^3 \text{ ha}^{-1}$, with a few exceptions (Figure 7), which included areas with high-SV coniferous forests along forest roads in the eastern part of the mapping area. SV was rather small in large portions of the study site, and SV was consistently low in hinoki cypress and deciduous broadleaved forests (Table 1). Regarding TDB, distribution (Figure 8) was slightly different from that of SV. The maximum of TDBs were similar among Japanese cedar, hinoki cypress, and deciduous broadleaved forests (Table 1), and TDB was more evenly distributed than SV in the study site.

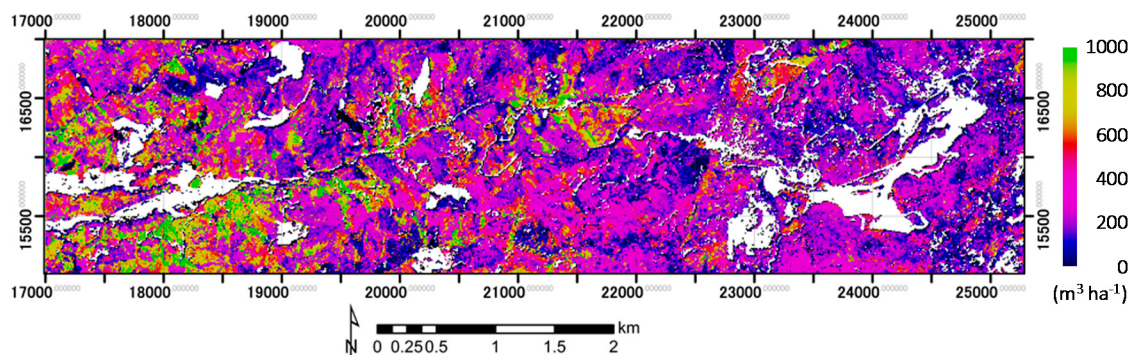


Figure 7. Distribution of SV using Equations (5) and (7). The white areas are non-forested.

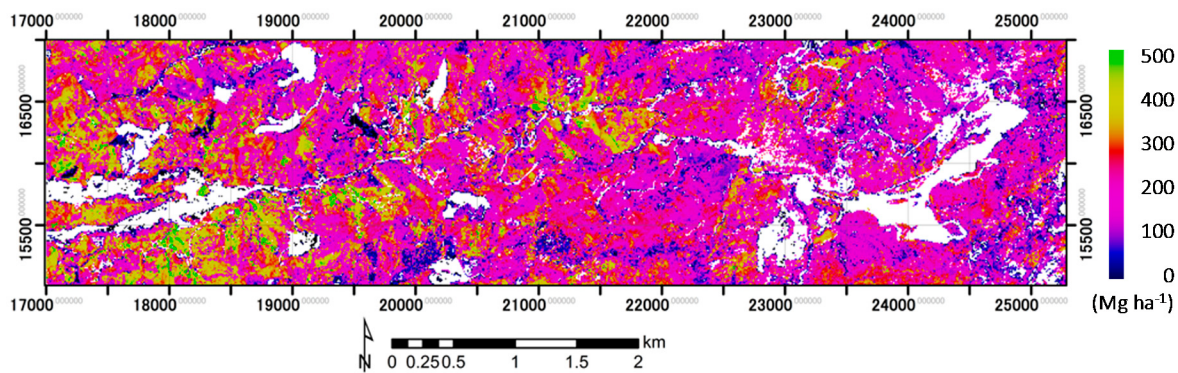


Figure 8. Distribution of TDB using Equations (2) and (8). The white areas are non-forested.

Frequency distributions were different between SV and TDB; the distribution of SV was right skewed; however, that of TDB was close to a normal distribution (Figure 9). The averages were 265.6 and 174.6 Mg ha⁻¹ for TDB and 280.5 and 224.3 m³ ha⁻¹ for SV for evergreen coniferous and deciduous broadleaved forests, respectively. Predicted SV and TDB were compared (Figure 10). The regression line in Figure 10 shows a relationship between predicted SV and predicted TDB of deciduous broadleaved forests. The relationship was different between broadleaved and conifer forests, with conifer stands having relatively greater SV than TDB as compared with broadleaved stands. The ratio of stem part of broadleaved forests are smaller than that of coniferous forests, and the ratio may be greater in mature than juvenile stands of coniferous forests. The difference between coniferous and deciduous broadleaved forests was larger in high-stock conifer stands; however, the reason was unclear.

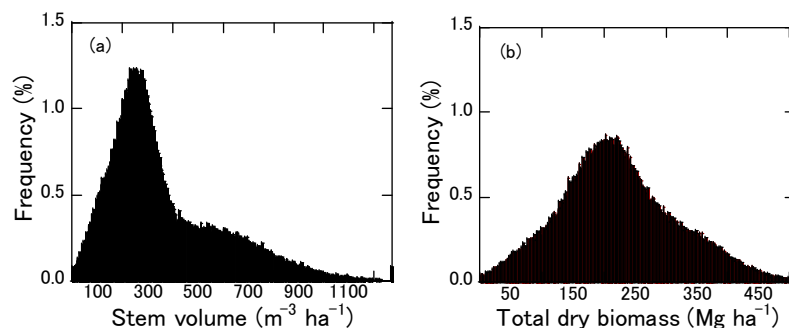


Figure 9. Frequency distributions of (a) SV and (b) TDB maps.

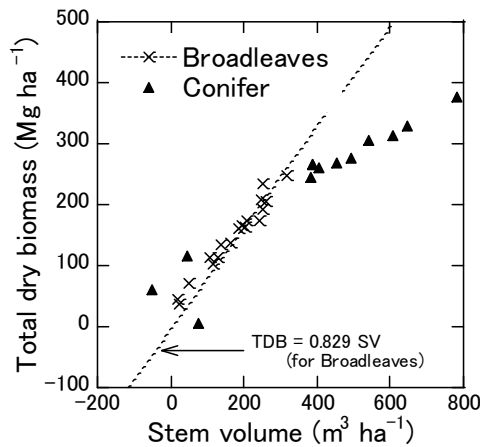


Figure 10. Comparison of predicted SV and TDB at validation plots.

4. Discussion

Sample size can impact statistical analyses. Therefore, sample selection is very important. We paid attention to the following components: (1) large numbers of samples are favorable for deriving stable results; (2) the impact that combining sample plots bears on statistical analysis; (3) the plot area should be sufficiently large to include enough number of trees which shows stand structure; and (4) minimizing the influence of DTM accuracy is important to evaluate the performance of LiDAR point data for TDB and SV estimation. We planned to measure plots as much as possible within a limited time. In order to reduce edge effects [5] and survey time, variable plot sizes were chosen, which included more than 40 trees. Survey areas were identified along forest roads using the aerial orthophotos. Futher, because of uneven age class distribution and small forest patch size in the study site, more forests in various tree sizes were selected. Sample plots were selected on graded slopes to reduce the influence of uncertain DTM accuracy.

The range of tree size and the combination of samples bear an impact on analyses. Therefore, forests with sizes ranging from very small to very great were surveyed to generalize results across coniferous and broadleaved forests in the study site. Selecting one plot from every three plots based on the order of TDB size, and combining them as three groups, made the tree size range and distribution similar among the three groups. If the sample size is small, statistical results can be greatly affected. We tried to maximize the number of samples by combining two groups for the regression analysis. The remaining plots were used to show the performance of the derived model independently from the regression analysis.

4.1. Correlations

The results showed that effective LiDAR variables differed by forest type (Tables 4 and 5). As for coniferous forests, AHavr showed the greatest score of the height variables by following other height variables, whereas only three mid-canopy heights showed similar scores for broadleaved forests. The difference between coniferous and deciduous forests is probably caused by different canopy structures. Regarding stand variables, AGB and TDB showed greater correlation coefficients than SV for coniferous forests; however, SV showed the best correlation for broadleaved forests. The specific gravity for dry biomass calculation was similar between Japanese cedar and hinoki cypress. The dry weight per unit volume was, therefore, almost identical between these species. Regarding parts of the tree used for biomass calculation, only the stem was included for SV, whereas the whole tree was included for TDB. This likely caused the observed differences in the correlation coefficients for SV and TDB (Tables 4 and 5). Additionally, broadleaved species have a wide range of specific gravity, and species composition changed widely among sample plots. The average canopy height is identical to the canopy space, which shows a linear relationship with SV [23], and probably TDB. However,

uneven specific gravity made TDB distribution uneven and caused worse correlation coefficients for AGB and TDB than for SV. Correlation coefficients were almost the same between AGB and TDB. Therefore, we suggest that the estimation of TDB could be as reliable as that of AGB, and AGB was, therefore, not analyzed thereafter.

4.2. Regression Analysis

Some studies reported coefficients of determination for SV of evergreen conifer stands that ranged between 0.887 and 0.97 [9,10,13,15]. The coefficient of determination of Equation (5) was 0.903 for SV of evergreen conifer stands, which is similar to those of the previous studies. Lim et al. [18] reported 0.931 as the coefficient of determination for the logarithmic estimation model for SV of broadleaved forest, and our study produced a value of 0.849 using the linear Equation (7). Although our value was smaller, logarithmic models tend to show greater coefficients of determination [10]. Therefore, our results may still be robust.

For the second variable, we selected no-height variables. The two-variable equations revealed that canopy structure variables, such as CHcv, CC, and C7, would be effective second variables for the estimation of SV and TDB. Since C8 was non-significant, the significance of the second variable was not high. When we applied an ordinary stepwise multiple regression analysis, height variables were mostly selected for the first and second variables. Two height variables could provide duplicate information for biomass estimation. Næsset [9], however, reported an SV estimation model with multiple height variables. In our cases, SEs in all one-variable equations were highly correlated with LiDAR height variables. The variation of variables, such as DBH, H, SV, TDB, and tree density, increases with stand age owing to both the uneven growth of individual trees and management operations, such as thinning. The size variation would be a function of age and, thus, canopy height. Therefore, LiDAR height variables probably correlated with variation in biomass among stands, related to the SEs in one-variable equations. Reducing SE was the greatest task to improve the accuracy of volume and biomass estimates, and the second height variable had an important role in the two-variable equations for reducing SE. Selecting two height variables could improve model accuracy; even if the first variable showed high correlation, the second variable would be meaningful without overfitting.

The validation results showed that there was substantial underestimation of SV for small stands, especially in one-variable models (Figure 5a). Stem volume and TDB are almost zero at an average canopy height of 1.2 m or less, since DBH, which is measured at that height, is zero. Using equations that pass through the origin are probably better to reduce estimation errors for small forests than using ordinary equations for biomass estimation. The large negative error was reduced by using the two-variable Equation (5) (Figure 5b). Correlation coefficients slightly improved by adding a second variable to the validation dataset. However, SEs became greater for SV and TDB of deciduous broadleaved forests. This indicated that the canopy height strongly affected the estimates, while the canopy structure variables did not affect the estimates significantly for deciduous broadleaved forests.

Standard errors of coniferous forest estimates were greater than those of deciduous broadleaved forests for SV and TDB (Figures 5 and 6). There were three possible reasons for this. First, although the canopy shape of Japanese cedar was different from that of hinoki cypress, and because of a lack of field plots of different age classes of each species and their planting history, we combined these data for the purpose of modeling. Therefore, the models were not best adapted to either Japanese cedar or hinoki cypress. Second, Japanese cedar and hinoki cypress forests were man-made. The thinning history, however, was very different among stands and, thus, the relationship between canopy height and SV or TDB was affected by different management histories. Finally, because broadleaved forests were native, the forests could maintain the greatest biomass and canopy height in the young stage. Canopy height and the variation of SV or TDB of broadleaved forests may be relatively smaller than those of coniferous forests. Validation of the cause is important to improve models.

4.3. Biomass Distribution

The spatial distributions of SV (Figure 7) and TDB (Figure 8) were quite different. TDB was more homogenously distributed than SV, and their frequency distributions were different, as shown in Figure 9. Figures 7 and 8 may, however, give a different impression to users regarding the biomass distribution. This is likely due to the difference in the proportion of stem to the entire tree between coniferous and broadleaved trees. The regression line in Figure 10 relates to the stem ratio of deciduous broadleaved trees. Coniferous forests showed a different trend from broadleaved forests.

The equations used for the calculation of SV [30–33] and TDB [34] for individual trees were produced in different ways. Equations were produced for each DBH size class for major tree species using numerous sample trees for SV. A common equation for TDB for all species was, however, produced. Additionally, differences in the modeling process suffers from the reliability of their samples. Although LiDAR height variables reflect spatial information and were similar to volume, TDB differs from volume because it reflects weight. This difference also influences the spatial distribution of the two biomass variables. Since high SV coniferous stands had relatively small TDB, the peak was broader in TDB than that in SV (Figure 9), which caused differences in the distribution patterns between SV and TDB (Figures 7 and 8).

SV and TDB are variables that are used in forestry [2]. The former is used for the trade of lumber, and the latter for the trade of biomass. TDB is also used in studies that evaluate ecosystem ecology and carbon production to help mitigate the effects of global warming [1,2]. However, different measures can yield different estimates, as shown in Figures 7 and 8. This study revealed that TDB would be a better measure than SV for conifer biomass mapping, and SV would be better than TDB for deciduous broadleaf biomass mapping owing to their higher model correlation coefficients and validation results compared to another variable (Figures 5 and 6).

5. Conclusions

Although this study builds on previous similar research [10,12–15], comparisons of coniferous and broadleaved forests or SV and TDB estimates, such as those presented herein, are scarce [21]. TDB and SV showed higher coefficients of determination in the coniferous forest models and the broadleaved forest models, respectively. The results suggest that TDB and SV are suitable variables for biomass mapping for coniferous and broadleaved forests, respectively, from the view point of correlation. However, the reason why a different biomass variable showed a better performance for coniferous or deciduous broadleaved forests was unclear. It is important to confirm this evidence in other forests and to identify the underlying causes in order to understand the meaning of LiDAR variables selected in statistical models. Stem, branch, and root ratios, and specific gravity used in the calculation of TDB, are likely the causes for the difference. Since statistical analyses cannot easily show deterministic mechanisms and root causes, utilizing any geometric tree model [39] would be necessary in future studies.

It has been recognized that stand-level analysis requires abundant plot data to produce empirical models for biomass estimates. Further, these models are often not transferable to other areas [38]. If DBH is measured or estimated, SV or AGB can be estimated using DBH and stem count density [40] or tree height [41]. Using equations for AGB estimation by single-tree-based approaches may be better than the stand-based approaches [41]. Our results will be transferrable to forests of the same species with a similar structure and the results will not be universal among various forests, as pointed out by other studies [5,38]. Forest structure varies greatly and is impacted, for example, by planting rates or thinning practices. Estimation errors could be larger in forests after thinning, since thinning changes the gap and tree distribution in various ways. This can resulted in changes in the relationship between biomass and LiDAR variables [38]. Although the first variable was almost the same in each forest type, the second variable was different. Standard errors of the two-variable equations were greater than those of the one-variable equations. These facts indicate that structural differences among the sample plot groups influences the second variable selection. The difference in stand structure, including

canopy height and variation, is especially influenced by thinning and must, therefore, be analyzed and included in prediction models to improve biomass estimates.

Forest plots were selected on graded slopes in order to reduce the influence of topography in this study. It was probably successful, since the correlation coefficient between the dominant tree height and CHavr was very high ($r = 0.987$). Steep and complex topography reduces the accuracy of biomass estimates using LiDAR-derived variables, since tree size is more variable on uneven terrain than graded slopes. However, topographic influence remains unclear in the biomass estimation. A precise DTM is necessary to reveal the influence of topography on stand-level biomass estimation using LiDAR data. Since forests exist on steep and complex mountain slopes in many parts of the world, the topographic effect on biomass estimation is an important issue.

Acknowledgments: This study was supported by JSPS KAKENHI (grant number JP22248017, “Development of validation method for the scaling up of carbon flux simulation using ecological process models”, Grant-in-Aid for Scientific Research A). The 2003 LiDAR data and three aerial orthophotos were provided by the Gifu Prefectural Government. The authors greatly appreciate field survey support from Mr. Kenji Kurumado (Takayama Research Center of Gifu University), Naoko Fukuda, and Hiroto Kawai (former Awaya Laboratory staff), and Siqinbilige Wang, Nabuti Alatan, and Weilisi (former Awaya Laboratory students). We give special thanks to the editor and the four anonymous reviewers for their valuable comments and suggestions on our manuscript.

Author Contributions: Yoshio Awaya designed the research and performed the field surveys, laser data processing, and statistical analysis; Tomoaki Takahashi provided mentorship for laser data processing and statistical analysis.

Conflicts of Interest: There was no conflict of interest between the two authors.

References

1. Food and Agriculture Organization of the United Nations (FAO). *Global Forest Resources Assessment 2015 How Are the World's Forests Changing?* 2nd ed.; FAO: Rome, Italy, 2016; pp. 1–44.
2. West, P.W. *Tree and Forest Measurement*, 2nd ed.; Springer: Berlin, Germany, 2009; pp. 22–63.
3. Arp, H.; Griesbach, J.C.; Burns, J.P. Mapping in Tropical Forests; A new approach using the laser APR. *PE&RS* **1982**, *48*, 91–100.
4. Aldred, A.H.; Bonner, G.M. *Application of Airborne Lasers to Forest Surveys (Inst. Information Report PI-X-51)*; Petawawa National Forestry: Petawawa, ON, Canada, 1985; pp. 1–62.
5. Næsset, E. Area-Based Inventory in Norway—From Innovation to An Operational Reality. In *Forestry Applications of Airborne Laser Scanning*; Maltamo, M., Næsset, E., Vauhkonen, J., Eds.; Springer: Dordrecht, The Netherlands, 2014; Volume 27, pp. 215–240.
6. Nelson, R.; Krabill, W.; Tonelli, J. Estimating forest biomass and volume using airborne laser data. *Remote Sens. Environ.* **1988**, *24*, 247–267. [[CrossRef](#)]
7. Lefsky, M.A.; Harding, D.; Cohen, W.B.; Parker, G.; Shugart, H.H. Surface lidar remote sensing of basal area and biomass in deciduous forests of eastern Maryland, USA. *Remote Sens. Environ.* **1999**, *67*, 83–98. [[CrossRef](#)]
8. Lefsky, M.A.; Cohen, W.B.; Acker, S.A.; Parker, G.C.; Spies, T.A.; Harding, D. Lidar remote sensing of the canopy structure and biophysical properties of Douglas-fir western hemlock forests. *Remote Sens. Environ.* **1999**, *70*, 339–361. [[CrossRef](#)]
9. Næsset, E. Estimating timber volume of forest stands using airborne laser scanner data. *Remote Sens. Environ.* **1997**, *61*, 246–253. [[CrossRef](#)]
10. Means, J.E.; Acker, S.A.; Fitt, B.J.; Renslow, M.; Emerson, L.; Hendrix, C.J. Predicting forest stand characteristics with airborne scanning lidar. *PE&RS* **2000**, *66*, 1367–1371.
11. Holmgren, J.; Nilsson, M.; Olsson, H. Estimation of tree height and stem volume on plots using airborne laser scanning. *For. Sci.* **2003**, *49*, 419–428.
12. Næsset, E.; Økland, T. Estimating tree height and tree crown properties using airborne scanning laser in a boreal nature reserve. *Remote Sens. Environ.* **2002**, *79*, 105–115. [[CrossRef](#)]
13. Næsset, E. Predicting forest stand characteristics with airborne scanning laser using a practical two-stage procedure and field data. *Remote Sens. Environ.* **2002**, *80*, 88–99. [[CrossRef](#)]

14. Næsset, E. Effects of different flying altitudes on biophysical stand properties estimated from canopy height and density measured with a small foot-print airborne scanning laser. *Remote Sens. Environ.* **2004**, *91*, 243–255. [[CrossRef](#)]
15. Magnusson, M.; Fransson, J.E.S.; Holmgren, J. Effects on estimation accuracy of forest variables using different pulse density of laser data. *For. Sci.* **2007**, *53*, 619–626.
16. Takahashi, T.; Yamamoto, K.; Senda, Y.; Tsuzuku, M. Estimating individual tree heights of sugi (*Cryptomeria japonica D. Don*) plantations in mountainous areas using small-footprint airborne LiDAR. *J. For. Res.* **2005**, *10*, 135–142. [[CrossRef](#)]
17. McCombs, J.W.; Roberts, S.D.; Evans, D.L. Influence of fusing LiDAR and multispectral imagery on remotely sensed estimates of stand density and mean tree height in a managed loblolly pine plantation. *For. Res.* **2003**, *49*, 457–466.
18. Lim, K.; Treitz, P.; Baldwin, K.; Morrison, I.; Green, J. Lidar remote sensing of biophysical properties of tolerant northern hardwood forests. *Can. J. Remote Sens.* **2003**, *29*, 658–678. [[CrossRef](#)]
19. Zhao, K.; Popescu, S.; Nelson, R. Lidar remote sensing of forest biomass: A scale-invariant estimation approach using airborne lasers. *Remote Sens. Environ.* **2009**, *113*, 182–196. [[CrossRef](#)]
20. He, Q.S.; Cao, C.X.; Chen, E.X.; Sun, G.Q.; Ling, F.L.; Pang, Y.; Zhang, H.; Ni, W.J.; Xu, M.; Li, Z.-Y. Forest stand biomass estimation using ALOS PALSAR data based on LiDAR-derived prior knowledge in the Qilian Mountain, western China. *Int. J. Remote Sens.* **2012**, *33*, 710–729. [[CrossRef](#)]
21. Cao, L.; Coops, N.C.; Hermosilla, T.; Innes, J.; Dai, J.; She, G. Using small-footprint discrete and full-waveform airborne lidar metrics to estimate total biomass and biomass components in subtropical forests. *Remote Sens.* **2014**, *6*, 7110–7135. [[CrossRef](#)]
22. Mora, B.; Wulder, M.A.; White, J.C.; Hobart, G. Modeling Stand Height, Volume, and Biomass from Very High Spatial Resolution Satellite Imagery and Samples of Airborne LiDAR. *Remote Sens.* **2013**, *5*, 2308–2326. [[CrossRef](#)]
23. Tsuzuki, H.; Kusakabe, T.; Sueda, T. Long-range estimation of standing timber stock in western boreal forest of Canada using airborne laser altimetry. *J. Jpn. For. Soc.* **2006**, *88*, 103–113. (In Japanese with English Summary) [[CrossRef](#)]
24. Kwak, D.; Lee, W.; Lee, J.; Biging, G.S.; Gong, P. Detection of individual trees and estimation of tree height using LiDAR data. *J. For. Res.* **2007**, *12*, 425–434. [[CrossRef](#)]
25. Takahashi, T.; Yamamoto, K.; Senda, Y.; Tsuzuku, M. Predicting individual stem volumes of sugi (*Cryptomeria japonica D. Don*) plantations in mountainous areas using small-footprint airborne LiDAR. *J. For. Res.* **2005**, *10*, 305–312. [[CrossRef](#)]
26. Kankare, V.; Vastaranta, M.; Holopainen, M.; Räty, M.; Yu, X.; Hyppä, J.; Hyppä, H.; Alho, P.; Viitala, R. Retrieval of forest aboveground biomass and stem volume with airborne scanning LiDAR. *Remote Sens.* **2013**, *5*, 2257–2274. [[CrossRef](#)]
27. Breidenbach, J.; McRoberts, R.E.; Astrupa, R. Empirical coverage of model-based variance estimators for remote sensing assisted estimation of stand-level timber volume. *Remote Sens. Environ.* **2016**, *173*, 274–281. [[CrossRef](#)] [[PubMed](#)]
28. Næsset, E.; Gobakken, T. Estimating forest growth using canopy metrics derived from airborne laser scanner data. *Remote Sens. Environ.* **2005**, *96*, 453–465. [[CrossRef](#)]
29. Forestry Agency of Japan. *Annual Report on Forest and Forestry in Japan Fiscal Year 2013*; Forestry Agency of Japan: Tokyo, Japan, 2014; p. 223. (In Japanese with English Summary)
30. Forestry Agency of Japan. *Description of Stem Volume Table Development for Manmade Sugi Cedar Stands in Nagoya Regional Forestry Office*; Forestry Agency of Japan: Tokyo, Japan, 1959; p. 17. (In Japanese)
31. Forestry Agency of Japan. *Description of Stem Volume Table Development for Manmade Hinoki Cypress Stands in Nagoya Regional Forestry Office*; Forestry Agency of Japan: Tokyo, Japan, 1959; p. 14. (In Japanese)
32. Forestry Agency of Japan. *Description of Stem Volume Table Development for Deciduous Broadleaved Stands in Nagoya Regional Forestry Office*; Forestry Agency of Japan: Tokyo, Japan, 1959; p. 19. (In Japanese with English Summary)
33. Forestry Agency of Japan. *Description of Stem Volume Table Development for Larch Stands in Nagoya Regional Forestry Office*; Forestry Agency of Japan: Tokyo, Japan, 1963; p. 29. (In Japanese with English Summary)

34. Komiya, A.; Nakagawa, M.; Kato, S. Common allometric relationships for estimating tree biomasses in cool temperate forests of Japan. *J. Jpn. For. Soc.* **2011**, *93*, 220–225. (In Japanese with English Summary) [[CrossRef](#)]
35. Fukuda, N.; Awaya, Y.; Kojima, T. Classification of forest vegetation types using LiDAR data and Quickbird images—Case study of the Daihachiga river basin in Takayama city. *J. JASS* **2012**, *28*, 115–122. (In Japanese with English Summary)
36. Fukuda, N.; Awaya, Y. Investigation of DTM generation using LiDAR data—A case in Daihachiga river basin. *Chubu For. Res.* **2013**, *61*, 107–108. (In Japanese)
37. Gaveau, D.L.A.; Hill, R.A. Quantifying canopy height underestimation by laser pulse penetration in small-footprint airborne laser scanning data. *Can. J. Remote Sens.* **2003**, *29*, 650–657. [[CrossRef](#)]
38. Rosette, J.; Suárez, J.; Nelson, R.; Los, S.; Cook, B.; North, P. Lidar Remote Sensing for Biomass Assessment. In *Remote Sensing of Biomass—Principles and Applications*; Fatoyinbo, T., Ed.; InTech: Rijeka, Croatia, 2012; pp. 3–26.
39. Ko, C.; Gunho Sohn, G.; Remmel, T.K.; Miller, J. Hybrid Ensemble Classification of Tree Genera Using Airborne LiDAR Data. *Remote Sens.* **2014**, *6*, 11225–11243. [[CrossRef](#)]
40. Yao, T.; Yang, X.; Zhao, F.; Wang, Z.; Zhang, Q.; Jupp, D.; Lovell, J.; Culvenor, D.; Newnham, G.; Ni-Meister, W. Measuring forest structure and biomass in New England forest stands using echidna ground-based lidar. *Remote Sens. Environ.* **2011**, *115*, 2965–2974. [[CrossRef](#)]
41. Maltamo, K.; Eerikäinenn, J.; Pitkänen, J.; Hyypä, M. Vehmas Estimation of timber volume and stem density based on scanning laser altimetry and expected tree size distribution functions. *Remote Sens. Environ.* **2004**, *90*, 319–330. [[CrossRef](#)]



© 2017 by the authors. Licensee MDPI, Basel, Switzerland. This article is an open access article distributed under the terms and conditions of the Creative Commons Attribution (CC BY) license (<http://creativecommons.org/licenses/by/4.0/>).